

Research Paper
Imaging

The anterior maxilla as a potential source of bone grafts: a morphometric cone beam computed tomography analysis of different anatomical areas

**R. Bernades Mayordomo,
R. Guijarro Martínez,
F. Hernández Alfaro**

Medicine, Surgery and Oral Implantology
Department, Dental School, Universitat
Internacional de Catalunya, Sant Cugat del
Vallès, Barcelona, Spain

R. Bernades Mayordomo, R. Guijarro Martínez, F. Hernández Alfaro: The anterior maxilla as a potential source of bone grafts: a morphometric cone beam computed tomography analysis of different anatomical areas. Int. J. Oral Maxillofac. Surg. 2016; 45: 1049–1056. © 2016 International Association of Oral and Maxillofacial Surgeons. Published by Elsevier Ltd. All rights reserved.

Abstract. The aim of this research was to use cone beam computed tomography (CBCT) to analyze the volume, density, and morphology of the bone available in the anterior region of the maxilla, in order to investigate its potential as a source of bone grafts. Three independent zones were evaluated: the palatine process of the maxilla (PPM), anterior nasal spine (ANS), and subnasal bone (SN). The latter was analyzed bilaterally (SN_R, SN_L). One hundred CBCT scans were evaluated. The morphometric analysis comprised volumetric and subsequent automatic density calculations, as well as linear measurements. Potential correlations among these parameters, including demographic characteristics, were investigated. The study comprised 52 women and 48 men (mean age 49.6 ± 14.5 years). The calculated bone volume averaged 2.41 ± 0.72 cm³ for PPM, 0.46 ± 0.16 cm³ for ANS, 0.58 ± 0.2 cm³ for SN_R, and 0.57 ± 0.21 cm³ for SN_L. The anterior region of the maxilla can provide a considerable amount of bone volume from different anatomical zones and should be regarded as a potential donor site for the regeneration of maxillary atrophic bones. Further investigation is required before these findings can be applied in the routine clinical setting.

Key words: bone graft; palatine process of the maxilla; anterior nasal spine; subnasal bone; CBCT; i-CAT; SIMPLANT; donor site.

Accepted for publication 1 March 2016
Available online 15 March 2016

The search for reliable bone graft donor sites is a constant aim of clinicians dedicated to oral and maxillofacial reconstruction. Although substantial investigation has resulted in the incorporation of several

allografts, xenografts, and alloplastic materials into the routine armamentarium, autologous bone grafting is still considered, in most cases, the gold standard option.^{1–4}

The reconstruction of certain maxillofacial defects requires clinicians to obtain autologous grafts from extraoral sites such as the iliac crest, tibia, and parietal bone. Alternatively, intraoral donor sites may be

preferable for certain indications in order to reduce morbidity, time, and costs.⁵ The disadvantage of these is that they often provide limited bone volume.^{5–7} In addition, the great variability that exists between individuals has been highlighted.^{8,9} Hence, an individualized analysis of each case is crucial.

Used in conjunction with the appropriate software, computed tomography (CT) provides the most powerful and reliable technique for pre- and postoperative assessment.¹⁰ However, the advent of cone beam computed tomography (CBCT) has provided a very convenient tool for the evaluation of the hard tissues in the dentomaxillofacial area. Advantages of CBCT include its wide accessibility, easy handling, and low radiation doses compared to conventional CT.¹¹

Unexpectedly, the number of studies assessing intraoral donor sites – even with conventional radiological techniques – is quite low.^{5,6,12,13} In fact, only one recent publication reports the combined use of CBCT and accurate volumetric measurements with a structured and reproducible method.¹⁴

Traditionally, the anterior region of the maxilla has been considered a recipient site for bone grafts. Very few studies have considered it as a donor site.^{15–18} To date, three different zones have been described for this purpose: the palatine process of the maxilla (PPM), anterior nasal spine (ANS), and subnasal bone (SN).

The present study investigators have recently described a specific methodology for the morphometric evaluation of the PPM using CBCT technology and a related third-party software.¹⁴ Based on the favourable preliminary results, the aim of this study was to assess the available bone volume, density, and morphology of the anterior region of the maxilla in a structured, precise, and reproducible way, and thereby to demonstrate its potential application as an alternative source of intraoral grafts.

Materials and methods

A retrospective analysis of the CBCT scans of 100 patients who had been referred to a university dental clinic for routine dental evaluation was performed. Patients were selected from the centre database according to the following inclusion criteria: CBCT imaging of the entire maxillary bone, complete physical growth (age ≥ 20 years), and dentate (from tooth 14 to 24). Patients with developmental malformations of the maxilla, tumours or cysts of the hard palate,

severe periodontitis involving the region from tooth 14 to 24, and impacted teeth in the area of study were excluded from further evaluation.

The study was conducted in accordance with the principles outlined in the Declaration of Helsinki (first adopted at the 18th World Medical Association General Assembly, Helsinki, Finland, June 1964). Ethical approval was obtained from the local ethics committee of clinical research. Written informed consent for CBCT analysis was obtained for each case. Patient confidentiality was safeguarded in compliance with the 15/1999 Organic Law. There was no direct or indirect contact with any of the study subjects, and their personal information was appropriately separated from the study database and filed for any possible audits, inspections, or confirmation of information veracity. Accordingly, each patient was assigned a number (consecutive from 1 to 100).

CBCT scans were obtained with an i-CAT device version 17–19 (Imaging Sciences International, Hatfield, PA, USA). The radiological parameters used were 120 kV and 5 mA; the axial slice default distance was 0.300 mm and the voxel size was 0.3 mm³. The facial mode with 23-cm field of view (FOV) was used. Primary images were stored as DICOM (Digital Imaging and Communication in Medicine) files.

The metric analysis was performed as described in a previous publication.¹⁴ This methodology was applied to each of the three anatomical regions studied: PPM, ANS, and SN. The patient's dataset was opened in SIMPLANT Pro 16.0 software (Materialise, Leuven, Belgium). The region of interest was defined in a sagittal slice view, eliminating all unnecessary areas. By default, the slice thickness was 0.3 mm. In order to obtain a thickness

per slice of 0.9 mm, two segments from each slice were omitted. In 'segmentation mode', a mask was created marking the starting point of the bone. All areas irrelevant to the study were again eliminated. Then, maximum quality was set for the three-dimensional (3D) analysis. Once in 'planning preparation mode', a panoramic curve was created to facilitate the readings on the different spatial planes. A ± 0.1 mm error deviation was established for all calculations. All measurements were taken from the axial plane in a caudal–cranial direction. Three references were set for each slice (anterior, posterior, and lateral margins). Once this protocol was implemented, a surface was created for each slice.

For the purpose of quantitative volumetric analysis, a 3D image of the delimited zone was constructed. Each of the three volumes of interest was defined as outlined below.

For the PPM, the starting slice was the base of the hard palate. The ending slice was the nasal floor. The anterior margin was the palatine area from tooth 14 to 24. This limit was defined by marking a point in the medial/palatine area of each tooth (Fig. 1). The same procedure was followed for the mesial and distal views wherever an adjacent tooth was not observed (usually in the longest canine roots) (Fig. 2). A 2-mm safety margin was established around the incisive canal. In this case, three peripheral points were marked (one on either side of the paramedials and one middle posterior). Similarly, a 2-mm safety margin was also set wherever the maxillary sinus appeared in the most cranial slices (Fig. 3). Wherever any of these teeth were no longer observed (usually in the most cranial slices), the anterior margin was delimited by the facial buccal plate. The posterior margin was the palatal

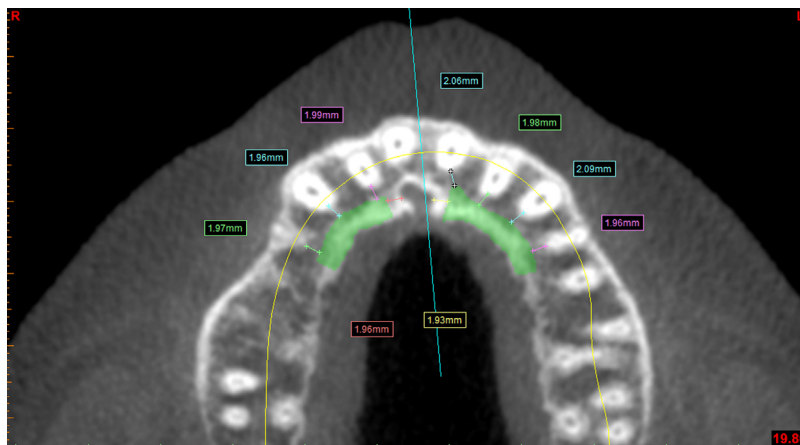


Fig. 1. Palatine process of the maxilla: axial caudal slice.

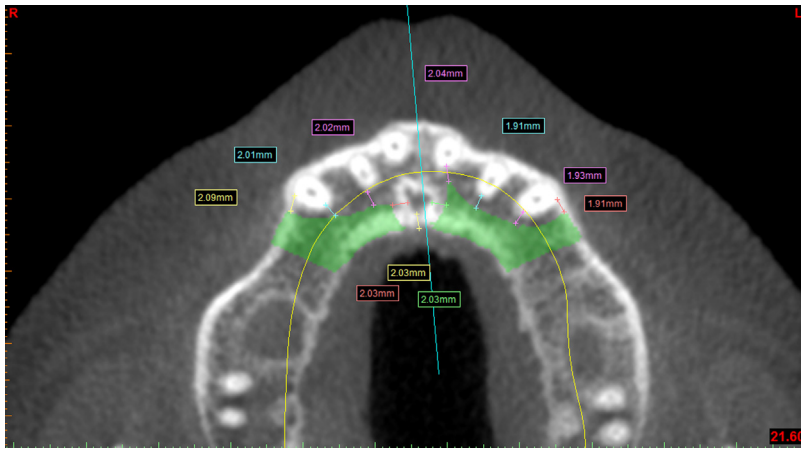


Fig. 2. Palatine process of the maxilla: axial middle slice.

vault (never beyond 14 and 24) and the lateral margins were projected lines in the distal area of 14 and 24.

For ANS, the starting slice was 2 mm above the apices of the upper central incisors (UCI). The ending slice was the nasal floor. The anterior margin was the

facial buccal plate, the posterior margin was 2 mm anterior to the incisive canal, and the lateral margins were projected lines 2 mm from both distal apices of the UCI (Fig. 4).

The SN area was assessed bilaterally (SN_R, SN_L). The starting slice was 2 mm

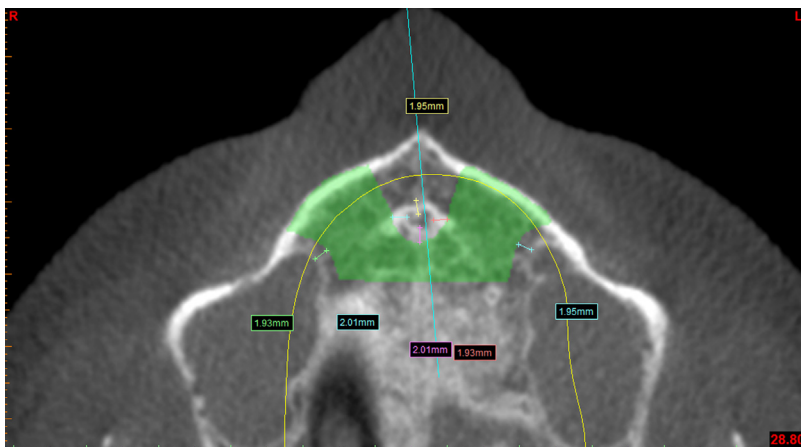


Fig. 3. Palatine process of the maxilla: axial cranial slice.

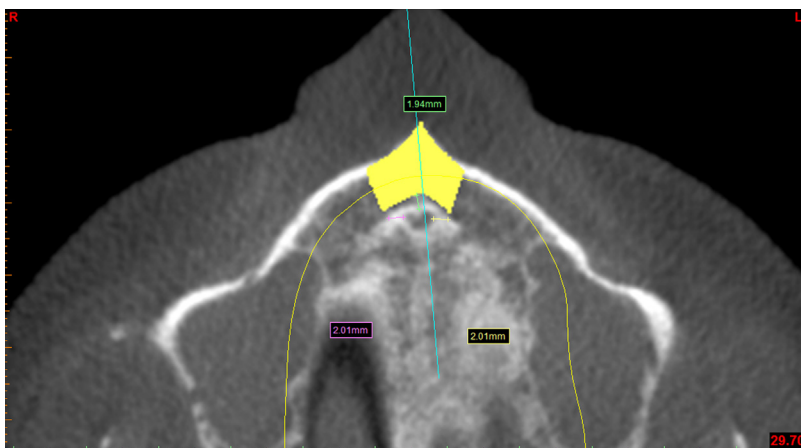


Fig. 4. Anterior nasal spine: axial middle slice.

above the apices of the upper lateral incisors (ULI). The ending slice was the nasal floor. The anterior margin was the facial buccal plate, the posterior margin was the posterior bony margin of the palatal vault (never beyond 14 and 24), and the lateral margins were projected imaginary lines from the distal apices of the ULC to the mesial apices of the upper canines (UC). A 2-mm safety margin was also set between these teeth (Figs 5 and 6).

After volume calculation, the mean density of each volume of interest was calculated automatically by the software.

Linear measurements were also performed in order to facilitate better understanding of the areas. These were outlined as follows: (1) For PPM, the height was the distance from the most caudal to the most cranial slice. (2) For ANS, the height was the distance from 2 mm above the apices of the UCI to the nasal floor. The width was the distance from 2 mm distal to the apex of the right UCI to 2 mm distal to the apex of the left UCI; the starting point was 2 mm above the apices of the UCI. The depth was the minimum distance from the incisive canal to the facial buccal plate; the starting point was 2 mm above the apices of the UCI. (3) For SN, the height was the distance from 2 mm above the apices of the ULI to the nasal floor. The width was the distance from 2 mm distal to the UCI to 2 mm mesial to the UC; the starting point was 2 mm above the apices of the ULI. The depth was the distance from the facial buccal plate to the posterior bony margin of the palatal vault (never beyond 14–24); the starting point was 2 mm above the apices of the ULI.

All measurements were submitted to statistical analysis using SPSS version 15.01 software (SPSS Inc., Chicago, IL, USA). A paired *t*-test was used to assess the degree of similarity between SN_R and SN_L. Pearson's linear correlation was used to study potential correlations among the different variables and all the areas studied. A multiple linear regression test was conducted to explain relationships between individual demographic characteristics and the volumes and densities of the three areas studied.

Results

The study sample comprised 52 women and 48 men with a mean age of 49.6 ± 14.5 years. Application of a Kolmogorov–Smirnov test confirmed the normality of the sample distribution (*P* > 0.200). Figures 7–9 display the mean volume, linear, and bone density measurements obtained for

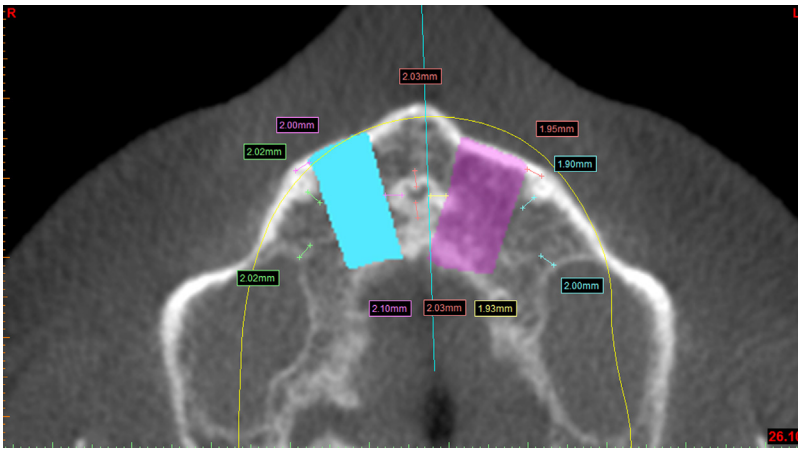


Fig. 5. Subnasal bone: axial middle slice.

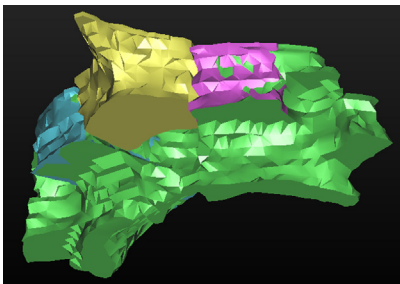


Fig. 6. Total volume reconstruction in 3D: oblique view.

the PPM, ANS, SN_R, and SN_L. Table 1 shows the results of paired *t*-tests for the comparison of SN_R and SN_L, which revealed a very high degree of symmetry.

High correlation coefficients were found among the different variables (volumes and densities) and different areas studied (Table 2). Figures 10 and 11 display the results of the analysis of potential relationships between individual demographic characteristics and the volumes and densities of the three

areas studied. Volumes showed different patterns and, conversely, densities reflected independency from age and sex for all areas analyzed.

Discussion

Despite clinical experience supporting the efficiency and reliability of the PPM as a potential donor site for the 3D reconstruction of alveolar defects,¹⁸ it was not until 2013 that a systematic method for analyzing an intraoral donor site using CBCT with suitable software was available.¹⁴

The selection of the ideal intraoral donor site should be based on several variables: location, quantity, quality, graft morphology, and possible intra- and post-operative complications.¹⁹ Taking these factors into account, the PPM shows a number of advantages, such as location, size, and type of graft. The most appropriate indication for a PPM graft is probably the regeneration of the anterior maxilla, because there is only one surgical field required and the surgical time and morbidity are significantly decreased.¹⁸

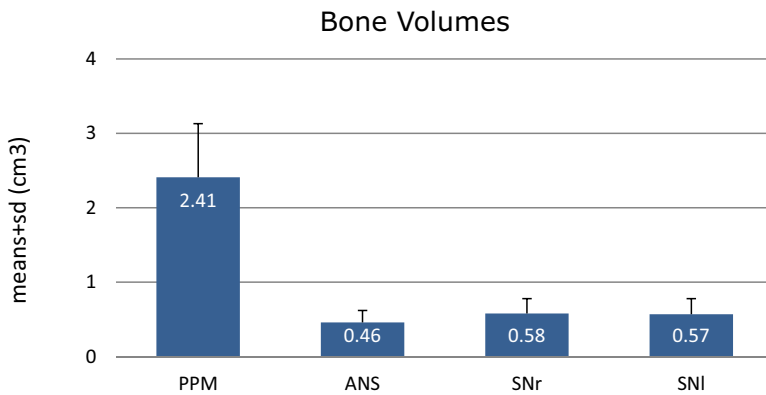


Fig. 7. Bone volumes (means and standard deviations) for the palatine process of the maxilla (PPM), anterior nasal spine (ANS), and subnasal bone (right, SN_R; left, SN_L).

Although implant therapy in the anterior maxilla is common, as is the need to regenerate this area,²⁰ to the authors' knowledge only three papers using the PPM graft method are available in the scientific literature. Together these add up to only 20 cases.^{18,21,22}

According to Agbaje et al.,²³ the mean socket volume from tooth 14 to 24 is $0.23 \pm 0.12 \text{ cm}^3$. Considering that the mean PPM graft in the previous pilot study¹⁴ measured $2.41 \pm 0.785 \text{ cm}^3$, it was inferred that the reliability of the PPM as a donor site for restoring proximal alveolar defects was justified quantitatively. In the present study, the application of a similar methodology to a wider sample confirmed the former findings; in fact, the results were extremely similar ($2.41 \pm 0.72 \text{ cm}^3$).

Considering these results, the amount of bone that can be grafted from the PPM is similar to that from the mandibular ramus,¹³ which is a well-established donor site. Moreover, the PPM provides intramembranous and corticocancellous bone. Reduced accessibility and the risk of damaging the neighbouring roots or causing nasal and sinus perforations are considered its major drawbacks.²¹ The description of safe zones for bone harvesting could help reduce such complications. Accordingly, different linear measurements have been included in this new research to facilitate better understanding of these areas (Fig. 8). The PPM was found to have an average height of $11.17 \pm 1.94 \text{ mm}$. These considerable dimensions could make this donor site a particularly good option for the regeneration of vertical bone defects.¹⁸ PPM width and depth were not assessed, because setting specific anatomical landmarks was found to be too arbitrary and clinically irrelevant, taking into account the individual characteristics of the palatal vault and the presence of the incisive canal.

No previous publications assessing the bone volume in this area were found. The present study quantitatively assessed the ANS in a structured, reproducible way, combining CBCT technology and a related third-party software. This was also the case for the analysis of the SN region.

In a clinical series of 15 cases, Cho et al. evaluated the postoperative effects of bone harvesting from the ANS on the overall nasal shape.¹⁷ The authors claimed that a block graft of $0.25\text{--}0.5 \text{ cm}^3$ volume could be harvested easily from this area. Unfortunately, the absence of a methodological explanation limits the validity and subsequent applicability of their findings.

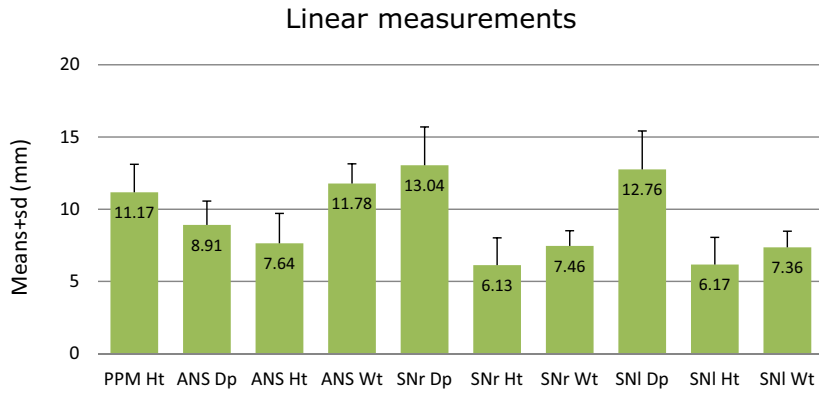


Fig. 8. Linear measurements (means and standard deviations) for the palatine process of the maxilla (PPM), anterior nasal spine (ANS), and subnasal bone (right, SNr; left, SNI) (Ht, height; Dp, depth; Wt, width).

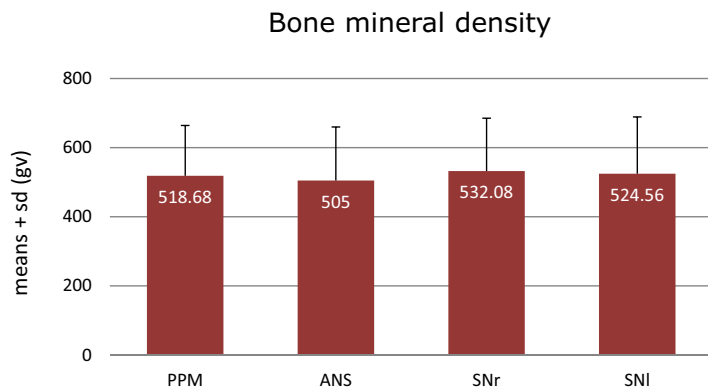


Fig. 9. Bone densities (means and standard deviations) for the palatine process of the maxilla (PPM), anterior nasal spine (ANS), and subnasal bone (right, SNr; left, SNI).

Conversely, the present study used a methodology that had been validated previously.¹⁴ In addition, a substantially greater sample size was evaluated. It can be inferred that the present results are therefore more accurate and reliable (mean volume $0.46 \pm 0.16 \text{ cm}^3$).

Regarding linear measurements, a depth of $8.91 \pm 1.65 \text{ mm}$ was obtained. This

measurement corresponds to the minimum distance between the facial buccal cortex and the incisive canal, since it was taken in its most caudal portion. As Thakur et al. observed in a series of 100 cases, the incisive foramen was always anterior to the nasopalatine foramen, indicating a posterior inclination of the incisive canal in all cases.²⁴

Mean height and width were $7.64 \pm 2.07 \text{ mm}$ and $11.78 \pm 1.36 \text{ mm}$, respectively. These data suggest that bone blocks of $7 \times 11 \times 9 \text{ mm}$ (height \times width \times depth) could commonly be harvested from this area without damaging the teeth or nasopalatine neurovascular bundle. Taking these dimensions into account, together with its anatomical location and buccal approach for surgical access, the ANS graft is probably a recommendable option for the restoration of small, local bone defects.

According to Yeung¹⁵ and Peñarrocha et al.,²⁵ only a 2–3 mm bone plug can be harvested from the SN region with a trephine bur. No further data are available in the scientific literature.

In the present research, the SN area was assessed bilaterally. Metric results (linear, volumetric, and densitometric) showed a very high degree of symmetry between SN_R and SN_L at all levels (Table 1). The statistical analysis revealed one significant difference only, related to the linear depth ($13.04 \pm 2.66 \text{ mm}$ for SN_R vs. $12.76 \pm 2.66 \text{ mm}$ for SN_L; $t = 2.51$; $df = 99$; $P = 0.014$). Nevertheless, it should be noted that this is a sub-millimetre difference and therefore of little clinical relevance.

Volume values averaged $0.58 \pm 0.20 \text{ cm}^3$ and $0.57 \pm 0.21 \text{ cm}^3$ for SN_R and SN_L, respectively. As a result, it can be inferred that a graft of approximately 1 cm^3 can be harvested with a dual buccal approach.

Linear measurements indicate that bone blocks measuring $6 \times 7 \times 13 \text{ mm}$ (height \times width \times depth) can be harvested from this area. Compared to the results provided by Yeung¹⁵ and Peñarrocha et al.,²⁵ the present findings suggest that a considerably larger graft is obtainable from the SN, and hence show this region to be a much more attractive source of bone grafts. At any rate, the SN graft is a variant of the PPM graft but with a vestibular approach, which implies improved accessibility. This is precisely one of the reported drawbacks of the PPM graft according to several authors.^{18,21}

High correlation coefficients were found among the volumes of the three studied areas (Table 2). In particular, the correlation between the PPM and the SN was especially high ($r = 0.744$; $P < 0.001$). This is quite a predictable relationship, since the SN graft comprises a portion of the PPM graft.

The correlation between demographic characteristics and different bone volumes was also investigated. Relationships were more evident in the PPM (analysis of

Table 1. Degree of symmetry between subnasal bone, right and left.

	Subnasal bone, right	Subnasal bone, left	P-value
Volume, cm^3	0.58 ± 0.20	0.57 ± 0.21	0.26
Depth, mm	13.04 ± 2.66	12.76 ± 2.66	0.014 ^a
Height, mm	6.13 ± 1.89	6.17 ± 1.88	0.387
Width, mm	7.46 ± 1.05	7.36 ± 1.12	0.257
Density, gv	532.08 ± 152.88	524.56 ± 164.28	0.185

^a Significant at $P < 0.05$.

Table 2. Correlations among palatine process of the maxilla (PPM), anterior nasal spine (ANS), and subnasal bone (SN) for volume and density.

	PPM–ANS	PPM–SN	ANS–SN
Volume	$r = 0.527$	$r = 0.744$	$r = 0.612$
Density	$r = 0.798$	$r = 0.942$	$r = 0.827$

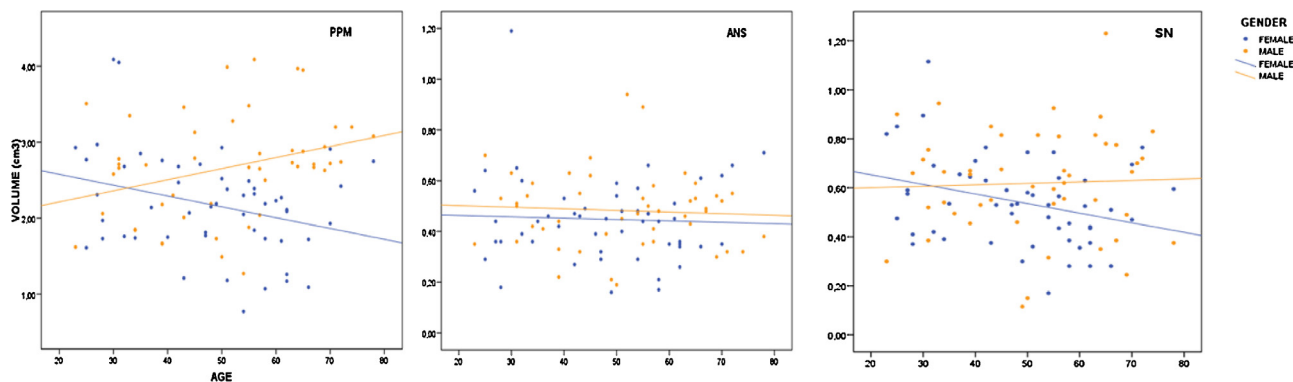


Fig. 10. Relationships between individual demographic characteristics and volumes for the palatine process of the maxilla (PPM), anterior nasal spine (ANS), and subnasal bone (SN).

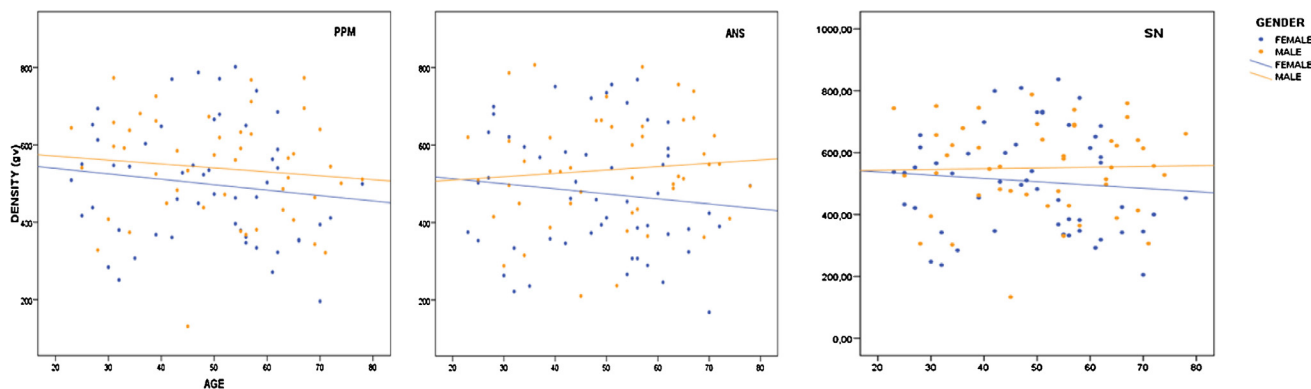


Fig. 11. Relationships between individual demographic characteristics and densities for the palatine process of the maxilla (PPM), anterior nasal spine (ANS), and subnasal bone (SN).

variance (ANOVA), $F = 8.16$; $df = 3$; $P < 0.001$), with a clear loss of volume in women with increasing age ($t = 3.18$; $P = 0.002$). On the other hand, a progressive volumetric gain was suggested for men. Age was the only variable that introduced a statistically significant difference longitudinally between the two sexes. In the SN area, males exhibited greater volume regardless of age, and females showed a recessionary trend as well. In the ANS, complete homogeneity was observed by sex and age (ANOVA, $F = 0.46$; $df = 3$; $P = 0.710$).

The densitometric analysis revealed very similar results for the different regions studied. In fact, density showed a very high degree of correlation (Table 2). It is noteworthy that the statistical models concluded that density was independent of age and sex for all areas analyzed. These results differ from the classic female trend of bone mineral density loss with age.

It must be noted that CBCT cannot be considered the imaging technique of choice for the evaluation of bone density.²⁶ This is due to the inherent

incapability of CBCT to provide Hounsfield unit (HU) measurements, since scanned regions of the same density in the skull can have different grey-scale values in the reconstructed CBCT dataset.^{27–29} However, substantial efforts have been made to address the lack of reliability of such results.^{30–34} Moreover, some authors have claimed that grey-scale values in CBCT may sometimes be comparable to real HU.^{30,31,35–39} Consequently, the mean bone mineral density of the anterior region of the maxilla can be estimated to be analogous to category D3 in the Misch classification.

Furthermore, the method error was not assessed for the different volume definitions. Evaluating intra-observer reliability could have added value to the present study, since the radiological boundaries used are not rigid anatomical landmarks.

Further limitations of this study are grounded in the fact that the purpose of the investigation was basic and not applied. Using a systematized, reproducible procedure, three anatomical zones with a limited literature context were evaluated

as potential donor sites for intraoral bone grafts. Although the primary objective of the study was achieved, further research is needed to answer the numerous clinical questions that derive from the application of this methodology. These questions include the definition of the best surgical approach, and the most suitable means of obtaining the graft according to the type of defect (saw vs. trephine vs. piezoelectric surgery; bone block vs. particulated graft). In addition, the metric contributions of this study could help define safety zones for bone graft harvesting in the anterior region of the maxilla and hence minimize risks and complications.

In conclusion, the results of this study suggest that the anterior region of the maxilla comprises several alternative grafting options that provide considerable bone volume. The quantity and quality of bone grafts that can be obtained from this region are similar or even superior to those of bone grafts from other intraoral donor sites. Thus, this area can be reliably regarded as a potential donor site for the regeneration of atrophic alveolar defects.

Funding

None.

Competing interests

None.

Ethical approval

Ethical approval was obtained from the Ethics Committee of Clinical Research (CEIC) of the Universitat Internacional de Catalunya (study number CIR-ELM-2014-01, approved 10/03/2014).

Patient consent

Not required.

References

- Pistilli R, Felice P, Piatelli M, Nisii A, Barausse C, Esposito M. Blocks of autogenous bone versus xenografts for the rehabilitation of atrophic jaws with dental implants: preliminary data from a pilot randomised controlled trial. *Eur J Oral Implantol* 2014;**7**:153–71.
- Nkenke E, Stelzle F. Clinical outcomes of sinus floor augmentation for implant placement using autogenous bone or bone substitutes: a systematic review. *Clin Oral Implants Res* 2009;**20**:124–33.
- Klein MO, Al-Nawas B. For which clinical indications in dental implantology is the use of bone substitute materials scientifically substantiated. *Eur J Oral Implantol* 2011;**4**:11–29.
- Jensen SS, Terheyden H. Bone augmentation procedures in localized defects in the alveolar ridge: clinical results with different bone grafts and bone-substitute materials. *Int J Oral Maxillofac Implants* 2009;**24**:218–36.
- Kainulainen VT, Sándor GK, Clokie CM, Keller AM, Oikarinen KS. The zygomatic bone as a potential donor site for alveolar reconstruction—a quantitative anatomic cadaver study. *Int J Oral Maxillofac Surg* 2004;**33**:786–91.
- Montazem A, Valauri D, St-Hilaire H, Buchbinder D. The mandibular symphysis as a donor site in maxillofacial bone grafting: a quantitative anatomic study. *J Oral Maxillofac Surg* 2000;**58**:1368–71.
- Sindet-Pedersen S, Enemark H. Reconstruction of alveolar clefts with mandibular or iliac crest bone grafts: a comparative study. *J Oral Maxillofac Surg* 1990;**48**:554–8.
- Martínez C, Inzunza O, Vargas A. Analysis of the hard palate as a donor site for bone grafting. *Int J Morphol* 2007;**25**:289–94.
- Gahleitner A, Podesser B, Shick S, Watzek G, Imhof H. Dental CT and orthodontic implants: imaging technique and assessment of available bone volume in the hard palate. *Eur J Radiol* 2004;**51**:257–62.
- Khoury F, Antoun H, Missika P. *Bone augmentation in oral implantology*. Hanover Park, IL: Quintessence; 2007: 53–66.
- De Vos W, Casselman J, Swennen GR. Cone-beam computerized tomography (CBCT) imaging of the oral and maxillofacial region: a systematic review of the literature. *Int J Oral Maxillofac Surg* 2009;**38**:609–25.
- Hassani A, Khojasteh A, Shamsabad AN. The anterior palate as a donor site in maxillofacial bone grafting: a quantitative anatomic study. *J Oral Maxillofac Surg* 2005;**63**:1196–200.
- Güngörmüş M, Selim Yavuz M. The ascending ramus of the mandible as a donor site in maxillofacial bone grafting. *J Oral Maxillofac Surg* 2002;**60**:1316–8.
- Bernades-Mayordomo R, Guijarro-Martínez R, Hernández-Alfaro F. Volumetric CBCT analysis of the palatine process of the anterior maxilla: a potential source for bone grafts. *Int J Oral Maxillofac Surg* 2013;**42**:406–10.
- Yeung R. Simultaneous placement of implant and bone graft in the anterior maxilla: a case report. *Int J Oral Maxillofac Implants* 2004;**19**:892–5.
- Buser D, Chen ST, Weber HP, Belser UC. Early implant placement following single-tooth extraction in the esthetic zone: biologic rationale and surgical procedures. *Int J Periodontics Restorative Dent* 2008;**28**:441–51.
- Cho YS, Hwang KG, Park CJ. Postoperative effects of anterior nasal spine bone harvesting on overall nasal shape. *Clin Oral Implants Res* 2013;**24**:618–22.
- Hernández Alfaro F, Martí C, García E, Corchero G, Arranz C. Palatal core graft for alveolar reconstruction: a new donor site. *Int J Oral Maxillofac Implants* 2005;**20**:777–83.
- Silva FM, Cortez AL, Moreira RW, Mazzonetto R. Complications of intraoral donor site for bone grafting prior to implant placement. *Implant Dent* 2006;**15**:420–6.
- Bornstein MM, Halbritter S, Harnisch H, Weber HP, Buser D. Current indications and surgical procedures in implant dentistry. A retrospective 3-year analysis of 1206 patients receiving 1817 implants in a referring clinic. *Int J Oral Maxillofac Implants* 2008;**20**:1109–16.
- Hassani A, Motamedi MH, Tabeshfar S, Vahdati SA. The crescent graft: a new design for bone reconstruction in implant dentistry. *J Oral Maxillofac Surg* 2009;**67**:1735–8.
- Rodríguez-Recio O, Rodríguez-Recio C, Gallego L, Junquera L. Computed tomography and computer-aided design for locating available palatal bone for grafting: two case reports. *Int J Oral Maxillofac Implants* 2010;**25**:197–200.
- Agbaje JO, Jacobs R, Maes F, Michiels K, van Steenberghe D. Volumetric analysis of extraction sockets using cone beam computed tomography: a pilot study on ex vivo jaw bone. *J Clin Periodontol* 2007;**34**:985–90.
- Thakur AR, Burde K, Guttal K, Naikmasur VG. Anatomy and morphology of the nasopalatine canal using cone-beam computed tomography. *Imaging Sci Dent* 2013;**43**:273–81.
- Peñarocha M, García-Mira B, Martínez O. Localized vertical maxillary ridge preservation using bone cores and a rotated palatal flap. *Int J Oral Maxillofac Implants* 2005;**20**:131–4.
- Campos MJ, de Souza TS, Mota Júnior SL, Fraga MR, Vitral RW. Bone mineral density in cone beam computed tomography: only a few shades of gray. *World J Radiol* 2014;**6**:607–12.
- Swennen GR, Schutyser F. Three dimensional cephalometry: spiral multislice vs cone-beam computed tomography. *Am J Orthod Dentofacial Orthop* 2006;**130**:410–6.
- Katsumata A, Hirukawa A, Noujeim M, Okumura S, Naitoh M, Fujishita M, et al. Image artifact in dental cone-beam CT. *Oral Surg Oral Med Oral Pathol Oral Radiol Endod* 2006;**101**:652–721.
- Katsumata A, Hirukawa A, Okumura S, Naitoh M, Fujishita M, Arijji E, et al. Effects of image artifacts on gray-value density in limited-volume cone-beam computerized tomography. *Oral Surg Oral Med Oral Pathol Oral Radiol Endod* 2007;**104**:829–36.
- Mah P, Reeves TE, McDavid WD. Deriving Hounsfield units using grey levels in cone beam computed tomography. *Dentomaxillofac Radiol* 2010;**39**:323–35.
- Reeves TE, Mah P, McDavid WD. Deriving Hounsfield units using grey levels in cone beam CT: a clinical application. *Dentomaxillofac Radiol* 2012;**41**:500–8.
- Liu Y, Bäuerle T, Pan L, Dimitrakopoulou-Strauss A, Strauss LG, Heiss C, et al. Calibration of cone beam CT using relative attenuation ratio for quantitative assessment of bone density: a small animal study. *Int J Comput Assist Radiol Surg* 2013;**8**:733–9.
- Kachelriess M, Sourbelle K, Kalender WA. Empirical cupping correction: a first-order raw data pre-correction for conebeam computed tomography. *Med Phys* 2006;**33**:1269–74.
- Naitoh M, Aimiya H, Hirukawa A, Arijji E. Morphometric analysis of mandibular trabecular bone using cone beam computed tomography: an in vitro study. *Int J Oral Maxillofac Implants* 2010;**25**:1093–8.
- Parsa A, Ibrahim N, Hassan B, Motroni A, van der Stelt P, Wismeijer D. Reliability of voxel gray values in cone beam computed tomography for preoperative implant planning assessment. *Int J Oral Maxillofac Implants* 2012;**27**:1438–42.
- Parsa A, Ibrahim N, Hassan B, van der Stelt P, Wismeijer D. Bone quality evaluation at dental implant site using multislice CT, micro-CT, and cone beam CT. *Clin*

- Oral Implants Res* 2015;**26**:e1–7. <http://dx.doi.org/10.1111/clr.12315>.
37. Pittman JW, Navalgund A, Byun SH, Huang H, Kim AH, Kim DG. Primary migration of a mini-implant under a functional orthodontic loading. *Clin Oral Investig* 2014;**18**:721–8.
38. Cha JY, Kil JK, Yoon TM, Hwang CJ. Miniscrew stability evaluated with computerized tomography scanning. *Am J Orthod Dentofacial Orthop* 2010;**137**:73–9.
39. Naitoh M, Hirukawa A, Katsumata A, Arijji E. Evaluation of voxel values in mandibular cancellous bone: relationship between cone-beam computed tomography and multislice helical computed tomography. *Clin Oral Implants Res* 2009;**20**:503–6.

Address:
Ramon Bernades Mayordomo
Medicine
Surgery and Oral Implantology Department

Dental School
Universitat Internacional de Catalunya
Josep Trueta
s/n 08195
Sant Cugat del Vallès
Barcelona
Spain
Tel: +34 935042000;
Fax: +34 935042001
E-mail: dr.bernades@hotmail.es